International Journal of Nanomedicine

Dovepress
Taylor & Francis Group

Open Access Full Text Article

ORIGINAL RESEARCH

Lymph Node Exosomes Delivery Attenuates Myocardial Ischemia-Reperfusion Injury via Regulating PTEN-PI3K/Akt Pathway Mediated Myocardiocyte Apoptosis

Shuaihua Qiao[1,2,*], Baochuan Wu[3,*], Lin Chen[3], Lingyu Ma[1], Yi Wang[3], Biao Xu[1], Rong Gu[3]

[1]Department of Cardiology, Nanjing Drum Tower Hospital, Affiliated Hospital of Medical School, Nanjing University, Nanjing, Jiangsu Province, People's Republic of China; [2]School of Cardiovascular and Metabolic Medicine & Sciences, Faculty of Life Sciences & Medicine, King's College London, London, UK; [3]Department of Cardiology, Nanjing Drum Tower Hospital Clinical College of Nanjing University of Chinese Medicine, Nanjing, Jiangsu Province, People's Republic of China

*These authors contributed equally to this work

Correspondence: Rong Gu; Biao Xu, Department of Cardiology, Nanjing Drum Tower Hospital, Affiliated Hospital of Medical School, Nanjing University, No. 321 Zhongshan Road, Nanjing, Jiangsu Province, 210008, People's Republic of China, Tel/Fax +86-25-68182812, Email gurong.nju@163.com; xubiao62@nju.edu.cn

Background: Ischemia/reperfusion (I/R) injury following acute myocardial infarction (AMI) induces myocardial apoptosis. Exosomes from KLF2-overexpressing endothelial cells (KLF2-EXO) dampened the effects of I/R injury. The intra-lymph node drainage pathway provides an alternative method to study the therapeutic effects of exosomes. In this study, we explored the role of intra-lymph node injection of KLF2-EXO in myocardial I/R injury.

Method and Result: Exosomes were isolated from KLF2-overexpressing mouse coronary endothelial cell supernatant via gradient centrifugation. The mice were subjected to ischemia and reperfusion, and an appropriate dosage of KLF2-EXO was administrated via intra-inguinal lymph node injection. KLF2-EXO attenuated I/R injury and alleviated myocardiocyte apoptosis in heart tissue, and immunofluorescence staining indicated KLF2-EXO could be transferred into the heart. MiRNA-sequencing of KLF2-EXO implicated that miRNA-486-5p (miR-486-5p) was a potent candidate mediator that inhibited myocardiocyte apoptosis, and the miR-486-5p antagomir reversed the effect. Further bioinformatics analysis and confirmation experiments revealed that PTEN functions as a downstream target and that the PTEN- PI3K/Akt pathway participates in the regulation of cardiomyocyte apoptosis.

Conclusion: Our data demonstrated that intra-lymph node injection of KLF2-EXO attenuated myocardial I/R injury in mice by delivering miR-486-5p to target PTEN- PI3K/Akt pathway, which restrained myocardiocyte apoptosis. KLF2-EXO may serve as an alternative therapy for myocardial I/R injury.

Keywords: intra lymph node injection, Krüppel-like factor 2-overexpressing mouse coronary endothelial cells, exosomes, myocardial ischemia/reperfusion injury, myocardiocyte apoptosis, miRNA-486-5p

Introduction

Acute myocardial infarction (AMI) is a deadly disease worldwide due to decreased coronary blood flow, resulting in an insufficient oxygen supply to the heart.[1] Reperfusion therapy, including fibrinolytic drugs and percutaneous coronary intervention (PCI), for AMI patients can recover blood flow to the ischemic myocardium and thus reduce the infarct size.[2] However, reperfusion triggers further myocardial damage known as reperfusion injury.[3] The ischemia/reperfusion (I/R) process induces various cascade reactions, including myocardiocyte apoptosis, neutrophil and monocyte activation and recruitment, necrotic cell clearance, tissue repair, and so on.[4–6] Many studies have focused on exploring an effective

Received: 19 December 2024
Accepted: 4 April 2025
Published: 17 April 2025

Graphical Abstract

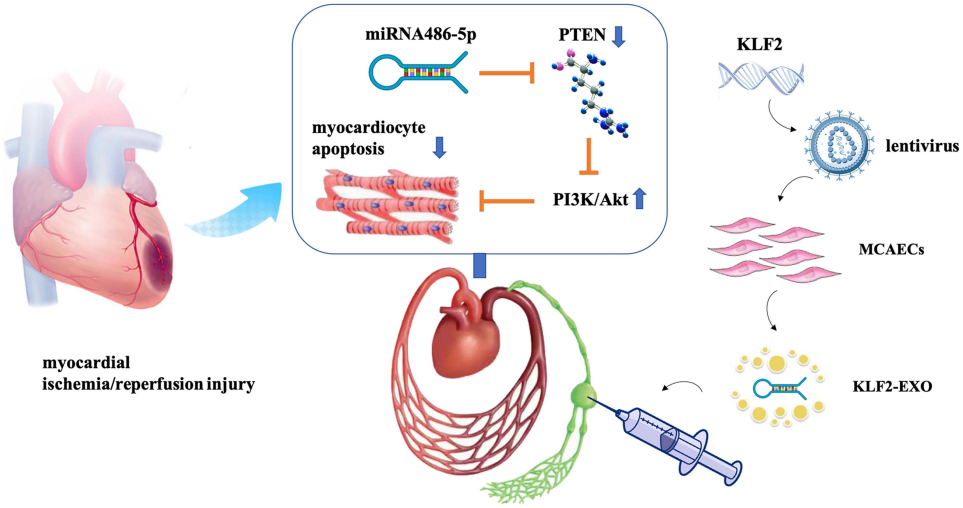

method to sustain an optimal but not an excessive inflammatory response.[7–9] Reducing myocardiocyte apoptosis is another way to repair the myocardium and improve its prognosis.[10]

Endothelial cells (ECs) play a vital role in vascular homeostasis as major functional coordinators.[11,12] Under pathological stress, ECs highly express Krüppel-Like Factor 2 (KLF2) through mechanosensory complex activation and adapt to laminar blood flow.[13] Previous studies have shown that KLF2-transduced ECs mediate monocyte/macrophage polarization during atherosclerosis.[14] However, the effect of KLF2-overexpressing endothelial cells on myocardial apoptosis following myocardial I/R injury remains unclear.

Exosomes, small particles with a diameter of approximately 50–150 nm, are potential biological mediators of therapeutic effects in diseases via their participation in intercellular communication.[15] Compared with cell therapy, exosomes have many benefits, including immunological inertness, nontoxicity, biocompatibility, escape from phagocytosis, and capacity to pass through biological barriers.[16] In a recent study, exosomes derived from KLF2-transduced ECs inhibited atherosclerotic lesion formation in the aortas of $ApoE^{-/-}$ mice.[14] Coincidentally, our previous study also indicated that extracellular vesicles derived from KLF2-transduced endothelial cells ameliorate myocardial I/R injury by inhibiting $Ly6C^{high}$ monocyte recruitment[9] and attenuating left ventricular dysfunction in a dilated cardiomyopathy (DCM) mouse model.[17] However, whether exosomes from KLF2-overexpressing ECs can reduce myocardial apoptosis in myocardial I/R injury remains to be explored.

The lymphatic system is part of the vertebrate immune system and is complementary to the circulatory system.[18] The lymph is a clear fluid in the lymphatic vessels back to the heart for recirculation, which transports cells and extracellular vesicles from the lymph nodes into the bones and heart.[19] The inguinal lymph nodes are in the groin area and are classified as superficial or deep; the former can be found after peeling within the femoral triangle in mice, and the latter is medial to the femoral vein. A Technetium-99 m radiolabelled nano colloid or blue dye is also often injected locally to assist with the visualization of nodes after incision.[20] Therefore, the inguinal lymph node-lymph-heart axis can be used to transport therapeutic exosomes. We chose intra-inguinal lymph node (iILN) injection over intracoronary (IC), intravenous (IV), or intramyocardial (IM) injections because of its operability and safety. However, the detailed mechanisms underlying the treatment of myocardial I/R injury with iILN injections remain elusive.

In this study, we isolated exosomes from KLF2-overexpressing mouse coronary endothelial cells (MCAECs) (KLF2-EXO), and injected them into mice after myocardial I/R injury. We found KLF2-EXO could restrain myocardiocyte

apoptosis and improve heart function, mediated via miRNA-486-5p (miR-486-5p) by targeting the PTEN- PI3K/Akt pathway.

Methods

Cell Experiments Protocol

The MCAECs were isolated from mouse coronary endothelium according to the protocol.[21] C57BL/6 mice were purchased (4 weeks of age) from the Model Animal Research Center of Nanjing University, and were injected intraperitoneally with 0.1 mL of Heparin to prevent blood coagulation and then were anesthetized by 1.5% isoflurane inhalation. Carefully isolate heart and put it into in a beaker with 1× Kreb's buffer. The heart tissue was digested with enzyme solution and conjugated with magnetic beads that took rat anti-mouse CD31 antibody. MCAECs were gained through magnetic activated cell sorting. MCAECs purity test was performed by staining cells with an endothelial cell surface marker CD31 and Dil-acLDL.

Exosomes Isolation and Characterization

MCAECs were cultured in endothelial cell culture medium (Cat #1001, ScienCell, San Diego, California, U.S.A). Exosomes were extracted by gradient centrifugation as previously described.[9] Exosome characterization was based on a general identification standard for exosomes.[22]

Animal Experimental Procedure

C57BL/6 mice at 8 weeks of age were bought from the Model Animal Research Center at Nanjing University. Mice were subjected to ischemia by surgically ligating the left anterior descending (LAD) coronary artery for 45 minutes, followed by reperfusion, as previously described.[8] Immediately after reperfusion, KLF2-EXO group mice were injected in inguinal lymph nodes with a total of 20 μL PBS containing KLF2-EXO at 1.5μg/g of body weight, and vector-EXO group mice were injected with an equal volume of vector-EXOs. The exosome dose was determined based on the results of a preliminary experiment.

Evans Blue and 2,3,5-Triphenyltetrazolium Chloride (Evans Blue/TTC) Staining

3 days following ischemia/reperfusion (I/R) injury, mice were anesthetized and the left anterior descending (LAD) coronary artery was re-occluded at the previous ligation and aorta was ligated at root, and then 0.1 mL of 1% Evans blue (Sigma-Aldrich, St. Louis, MO, USA) was injected into the left ventricular (LV) cavity. The heart was quickly excised, washed with normal saline and immediately frozen. Afterward, the heart tissue was cut in short-axis direction at 1 mm thickness and were incubated at 37°C in 1.5% 2,3,5-triphenyltetrazolium chloride (TTC; Sigma-Aldrich) for 15 minutes. The heart pieces were unfolded in glass slide and digitally photographed. LV area, areas at risk (AAR), and infarct size (IS) were determined by computerized planimetry and comprehensively analyzed in serial sections of each mice using Image J software (version 1.38, National Institutes of Health, Bethesda, MD, USA).

Histology

Histology of hearts was assessed on day 14 after myocardial I/R. Hearts were arrested in diastole late term with intraventricular injection of 10% potassium chloride (KCl). The heart was quickly excised, washed with normal saline and were fixed with 4% phosphate-buffered formalin. After gradually dehydration and embedded in paraffin, the tissue was cut into transverse sections at 5 μm thickness. For Masson trichrome staining, tissue slices were stained with Masson trichrome or Sirius red according to the manufacturer's instruction. To assess scar area, we digitally photographed the heart tissue slides and calculated the ratio of the collagen (blue-stained) area to the total tissue area. The collagen-rich border zone of the vessels was excluded from the analysis. For TUNEL staining, the deparaffinized tissue slides were boiled in citrate buffer at 100 °C for one hour for antigen retrieval and then were blocked in 1% FBS at room temperature for one hour followed by overnight incubation with primary antibodies at 4 °C. To determine apoptosis level of myocytes, we used a double staining with MHC antibody (Invitrogen, USA) and TUNEL (KeyGEN, China) in

conjunction with DAPI. Images were captured and processed using a fluorescence microscopy (IX 53, Olympus Corporation, Japan). Count and calculate separately MHC+TUNEL+ cells ratio in three fields (400× magnification) from four or five animals with each treatment.

Echocardiography

Cardiac function was evaluated professional technicians using Color Doppler Echocardiography (VEVO 1100 Imaging system; VisualSonics Inc). Mice were under light anesthesia and two-dimensional short and long axes imaging were acquired to calculate LV functional parameters. LV end-systolic diameter (LVID; d), LV end-diastolic diameter (LVID; s), interventricular septal thickness (IVS) and LV posterior wall thickness (LVPW) (end-diastolic and end-systolic) were measured from at least three consecutive cardiac cycles on the M-mode tracings. LV fractional shortening (FS) was determined as [(LVIDd–LVIDs)/LVIDd]× 100. LV ejection fraction (EF) was calculated as: EF (%) = ((LVVold-LV Vols)/LVVold) × 100. LVVold = ((7.0/(2.4 + LVIDd)) × LVIDd3); LVVols = ((7.0/(2.4 + LVIDs)) × LVIDs3).

Labelling of Exosomes with CM-DiL

To observe the transfer and distribution of the exosomes in vivo, exosomes were labelled with CM-DiL (Cat#C7000, Thermo Fisher Scientific, Waltham, Massachusetts, U.S.A) according to the manufacturer's instructions. Then the CM-DiL-labelled KLF2-EXOs (1.5 μg/g) were injected into the inguinal lymph nodes in I/R injury mice. After 72 hours, the inguinal lymph nodes, axillary lymph nodes and heart tissue were separated from mice and cut into tissue slides. The slides were photographed with a confocal microscope (FV1200, Olympus, Breinigsville, Pennsylvania, U.S.A) in conjunction with DAPI.

MicroRNA Microarray

Total mRNA in the exosomes was extracted using TRIzol® Reagent (Cat#15596026, Thermo Fisher Scientific, Waltham, Massachusetts, U.S.A) according to the manufacturer's protocol. RNA consistency was determined using a correlation plot. In the process of differentially expressed miRNA analysis, $|\log2(FC)| \geq 0.584962500721156$ and P value<=0.05 were used as screening criteria. In addition, considering that miRNAs expressed at low levels have little biological significance, we retained only those miRNAs with mean expression levels higher than 10 as the final set of differentially expressed miRNAs. Microarray analysis was performed using the edgeR software based on the miRBase database. Three duplicates of exosomes were included for each group.

Quantitative Reverse Transcriptase Polymerase Chain Reaction (qRT-PCR)

Total RNA was extracted from frozen or fresh tissues and cells with TRIzol® Reagent (Invitrogen) and reversely transcribed into cDNA with the Transcriptor First Strand cDNA Synthesis Kit (Roche LifeScience) to add polyA tail for miRNA. The expression levels of genes were quantified with the SYBR Green Reagents Kit (Roche LifeScience), and was normalized to that of the internal reference gene U6 to calculate the $2^{-\Delta Ct}$ value. Data were showed as the mean ± SD from at least three repeated experiments. The sequence of primers (5′ to 3′): miR-486-5p-forward: GCAGTCCTGTACTGAGCTG; miR-486-5p-reverse: GTCCAGTTTTTTTTTTTTTTCTCG; U6-forward: CGCTTCGGCAGCACATATAC; U6-reverse: AAATATGGAACGCTTCACGA. KLF2-forward: CTCAGCGAGCCTATCTTGCC; KLF2-reverse: CACGTTGTTTAGGTCCTCATCC.

Prediction of Target Genes and Dual-Luciferase Reporter Assay

We used TargetScan7.2 software to predict the potential target genes of miR-486-5p, and then divided these genes into different groups according to the results of the GO and KEGG analyses. A dual-luciferase reporter assay was used to confirm the interaction between miR-486-5p and tensin homolog (PTEN). The sequence of miR-486-5p is UCCUGUACUGAGCUGCCCCGAG. The mRNA sequence of the PTEN mRNA 3′-UTR segment (5′-ATATTTGTAGTGGGGTACAGGAATGAACCAT…3′) was amplified, and the corresponding cDNA segments were inserted into the pRL-TK vector (KeyGEN, Nanjing, Jiangsu, China). HEK293 cells were transfected with PTEN or NC vectors as well as miR-486-5p mimic or mimic-NC using Lipofectamine 2000 (Cat#11668030, Thermo Fisher

Scientific, Waltham, Massachusetts, U.S.A). Luciferase activity was detected and analyzed using the Dual-Luciferase® Reporter Assay System (Cat#N1610, Promega, Madison, Wisconsin, U.S.A) after 48 hours. Three replicates were performed for each group.

Western Blot

The total protein was extracted from tissue or cells and boiled with loading buffer for 5 minutes. Protein electrophoresis was conducted using TGX FastCast acrylamide Kit (BIO RAD Laboratories Inc)., and then transferred to PVDF membrane (Millipore, Bedford, MA, USA). After blocking in 5% dry milk, the membrane was incubated with primary antibodies (KLF2: Invitrogen, MA5-48691, 1:1000; Bax: Proteintech, 50599-2-Ig, 1:5000; Bcl2: Abmart, T40056F, 1:1000; PI3K: Abmart, T40115F, 1:1000; Phospho-PI3-kinase: Abmart, 1:1000; Phospho-Akt: Abmart, T40056F, 1:1000; AKT: Proteintech 10176-2-AP 1:5000; GAPDH: Proteintech, 10494-1-AP, 1:20,000; β-Tubulin: Proteintech, 10094-1-AP, 1:5000; Cleaved Caspase3: CST, 9661T, 1:1000). Next, the membrane was washed in Tris-buffered saline with Tween 20 (0.1%) (TBS-T) for least three times and was incubated with horseradish peroxidase-conjugated secondary antibodies (HRP-conjugated Goat Anti-Rabbit IgG(H+L): Proteintech, SA-00001-2, 1:10000; HRP-conjugated Goat Anti-Mouse IgG(H+L): Proteintech, SA-00001-1, 1:10,000). Detection was performed using ECL Prime (GE Healthcare, Logan, UT, USA) according to the manufacturer's instructions.

Recombinant Lentivirus Vector Assembly and Transduction into MCAECs

In the present study, we first constructed a GV358 vector (Ubi-MCS-3FLAG-SV40-EGFP-IRES-puromycin) carrying Krüppel-Like Factor 2 (KLF2) cDNA and was co-transfected with lentivirus backbone plasmid into HEK293A cells to produce the recombinant lentivirus vector Lv-KLF2. Another GV358 vector without KLF2 cDNA was used to generate empty viruses as controls (empty vector). ECs were cultured at a density of 1×10^6 cell/mL in six-well plates overnight. The lentiviruses (1.5×10^9 TU/mL) were diluted with 1 mL of complete medium containing HitransG P (1 μg/mL, GeneChem, China) and then added to MCAECs. After transfection for 12 hours at 37 °C, the medium was changed to fresh virus-free medium. Continually culturing for 72 hours, we could detect successfully transfected cells presented green fluorescence (GFP positive) with a fluorescence microscopy (IX 53, Olympus Corporation, Japan). Next, the puromycin (5 μg/mL) was applied to the culture medium to remove negative cells, and the selected cells were KLF2-transfected ECs. The KLF2 expression levels were measured by quantitative reverse transcriptase polymerase chain reaction (qRT-PCR) and Western blot.

Statistical Analysis

All values are presented as the mean ± standard deviation (SD) as appropriate. Statistical significance was measured using Student's *t*-test for two-group comparisons and one-way analysis of variance (ANOVA) followed by Tukey's multiple comparisons test for multiple-group comparisons. P values were considered statistically significant differences. All statistical analyses were performed using GraphPad Prism 9.0 (Graph Pad Prism Software, Inc., Boston, Massachusetts, U.S.A).

Results

Exosomes Were Isolated from KLF2-Transduced MCAECs

MCAECs were isolated from the coronary endothelium of C57BL/6 mice and stained with the endothelial cell surface markers CD31 (Figure 1A) and Dil-acLDL (Figure 1B) to confirm their purity. The percentage of MCAECs (CD31+ or Dil-acLDL+ cells) was > 90%. These results indicate that MCAECs were successfully isolated. We then transduced MCAECs with a lentivirus vector encoding KLF2 (KLF2-MCAECs), which resulted in a prominent increase in KLF2 expression at the mRNA and protein levels compared to those in non-sense lentiviral vector-transduced MCAECs (vector-MCAECs) (Figure 1C–F). Next, we cultured KLF2-MCAECs and vector-MCAECs, separately isolated exosomes (KLF2-EXO and Vector-EXO) from the culture supernatant via ultracentrifugation, and identified KLF2-EXO. Nanoparticle tracking analysis (NTA) showed that the diameters of the vesicles ranged from 50 to 150 nm (Figure 2A,

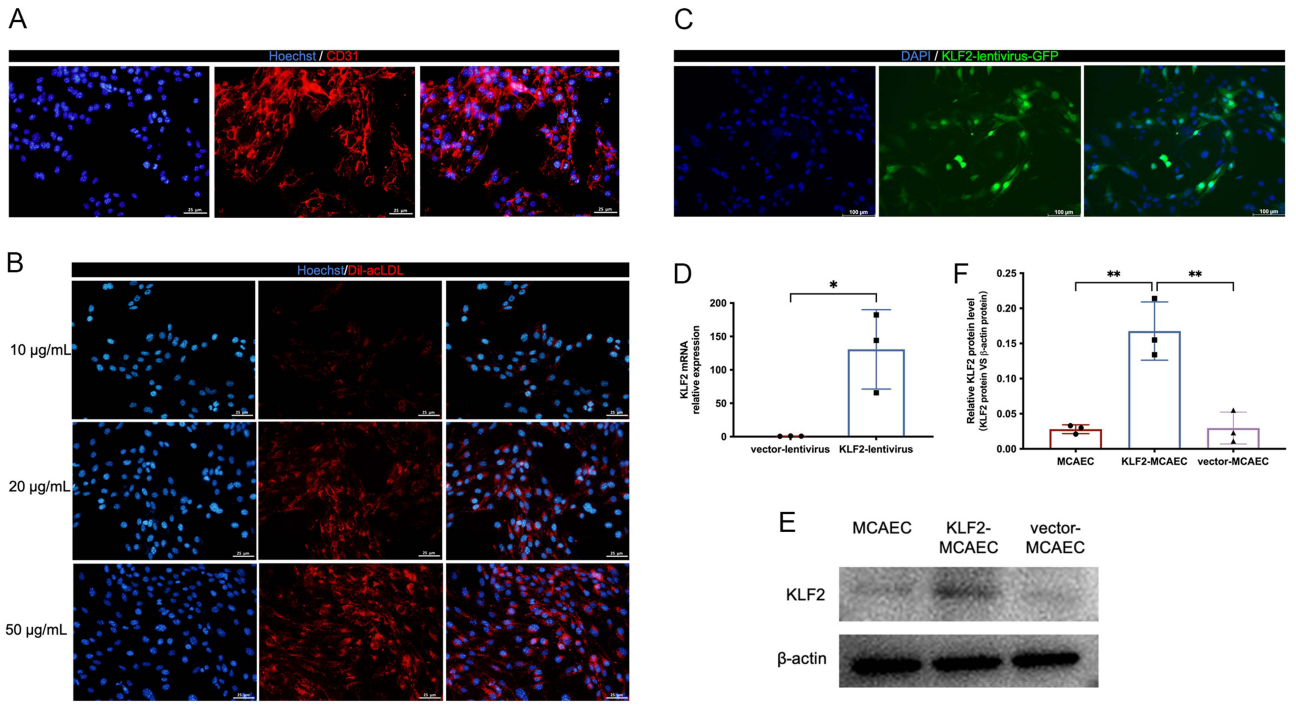

Figure 1 Overexpress KLF2 in mouse coronary endothelial cells (MCAECs) with a lentivirus vector. (**A**) Fluorescence images showing CD31 staining in red in MCAECs and Hoechst staining in blue in the nucleus. Scale bar=25μm. (**B**) Fluorescence images showing acLDL staining in red uptake in MCAECs at different concentrations of 10μg/L, 20μg/L and 50μg/L, and the nucleus stained with Hoechst in blue. Scale bar=25μm. (**C**) Representative fluorescence staining of KLF2 (green fluorescent protein) in KLF2-transduced MCAECs. Scale bar=100μm. (**D**) Quantification of KLF2 mRNA by qRT-PCR in KLF2-transduced MCAECs compared with empty vector-transduced MCAECs (n=3). (**E**) Representative images of Western blotting to assess KLF2 expression in KLF2-transduced MCAECs (KLF2-MCAEC), empty vector-transduced MCAECs (vector-MCAEC), and MCAECs. (**F**) Quantification of (**E**) (n=3). Graphs represent mean ± SD. Statistical significance was measured using Student's *t*-test for comparison between two groups and one-way ANOVA followed by Tukey's multiple comparisons test for multiple group comparisons. *P < 0.05, **P < 0.01.

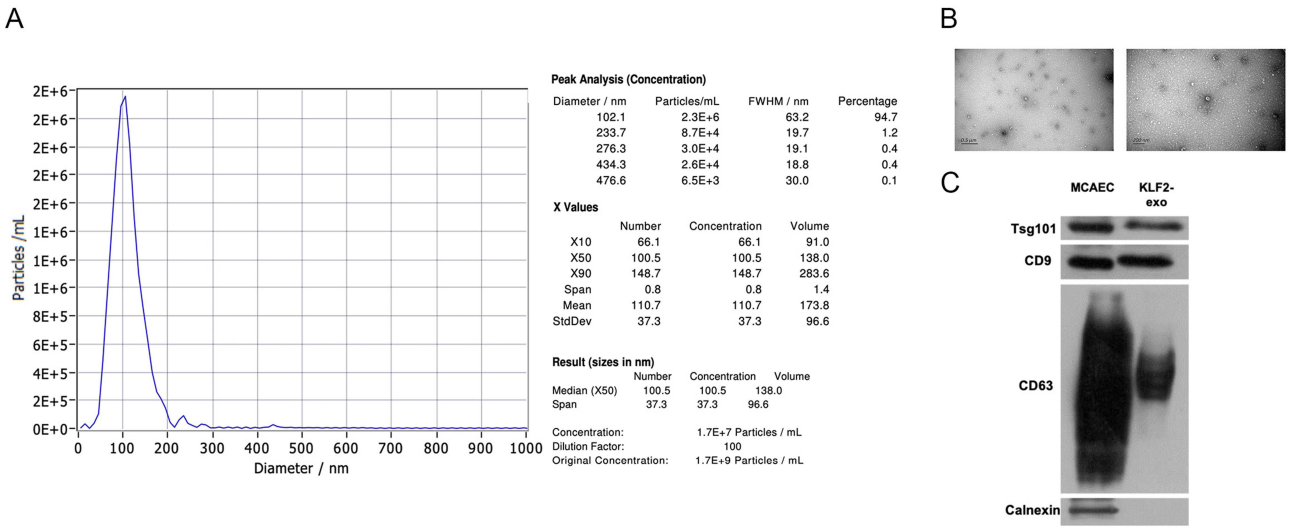

Figure 2 Exosomes were isolated from KLF2-transduced mouse coronary endothelial cells (MCAECs). (**A**) Nanoparticle trafficking analyzed the diameters and concentration of KLF2-EXO (KLF2-transduced MCAECs derived exosomes). (**B**) Transmission electron micrograph of KLF2-EXO. Scale bar=0.5μm/200 nm. (**C**) Representative images of Western blot to assess the presence of CD9, CD63, Tsg101 and Calnexin of KLF2-EXO.

Supplementary Material 1 for detailed data). Transmission electron microscopy (TEM) demonstrated that the vesicles had a cup-shaped canonical morphology and double-layer membrane structure, which is specific for exosomes (Figure 2B). Furthermore, Western blotting revealed that the extracellular vesicles expressed exosome markers, such as CD63, CD9, and Tsg101, and lacked the cellular debris protein calnexin (Figure 2C). These results confirm the

authenticity of the isolated particles as exosomes. Additionally, the protein concentration of the exosomes measured using BCA was strongly correlated with the number of exosomes measured using NTA. Thus, we used the BCA assay to quantify exosomes.

KLF2-EXO Attenuated Myocardial I/R Injury

To explore whether KLF2-EXO attenuated myocardial I/R injury, we surgically induced I/R injury in mice and injected KLF2-EXO or Vector-EXO into the inguinal lymph nodes immediately after reperfusion. Cardiac function was assessed using echocardiography (UCG) 3 and 14 days after myocardial I/R injury. We found that both the ejection fraction (EF) and fractional shortening (FS) were increased on day 3 and 14 in KLF2-EXO-treated mice compared with those in the vector-EXO -treated mice group (Figure 3A–F), indicating improved cardiac function. Evans blue/TTC staining was used to determine the extent of cardiac I/R injury on day three after reperfusion. Although the areas at risk (AAR) were similar, the infarct size (IS)/AAR ratio was significantly lower in KLF2-EXO-treated mice than in the control mice (Figure 3G–I). The heart was harvested after UCG administration on day 14 for histological assessment. Masson's trichrome staining revealed that KLF2-EXO reduced fibrosis area in the infarct zone (Figure 3J and K). Therefore, we concluded that KLF2-EXO attenuated myocardial I/R injury, including improved cardiac function, reduced infarct area, and alleviated fibrosis, compared with vector-EXOs. We investigated the mechanism underlying of KLF2-EXO′ effect on myocardial I/R injury in subsequent experiments.

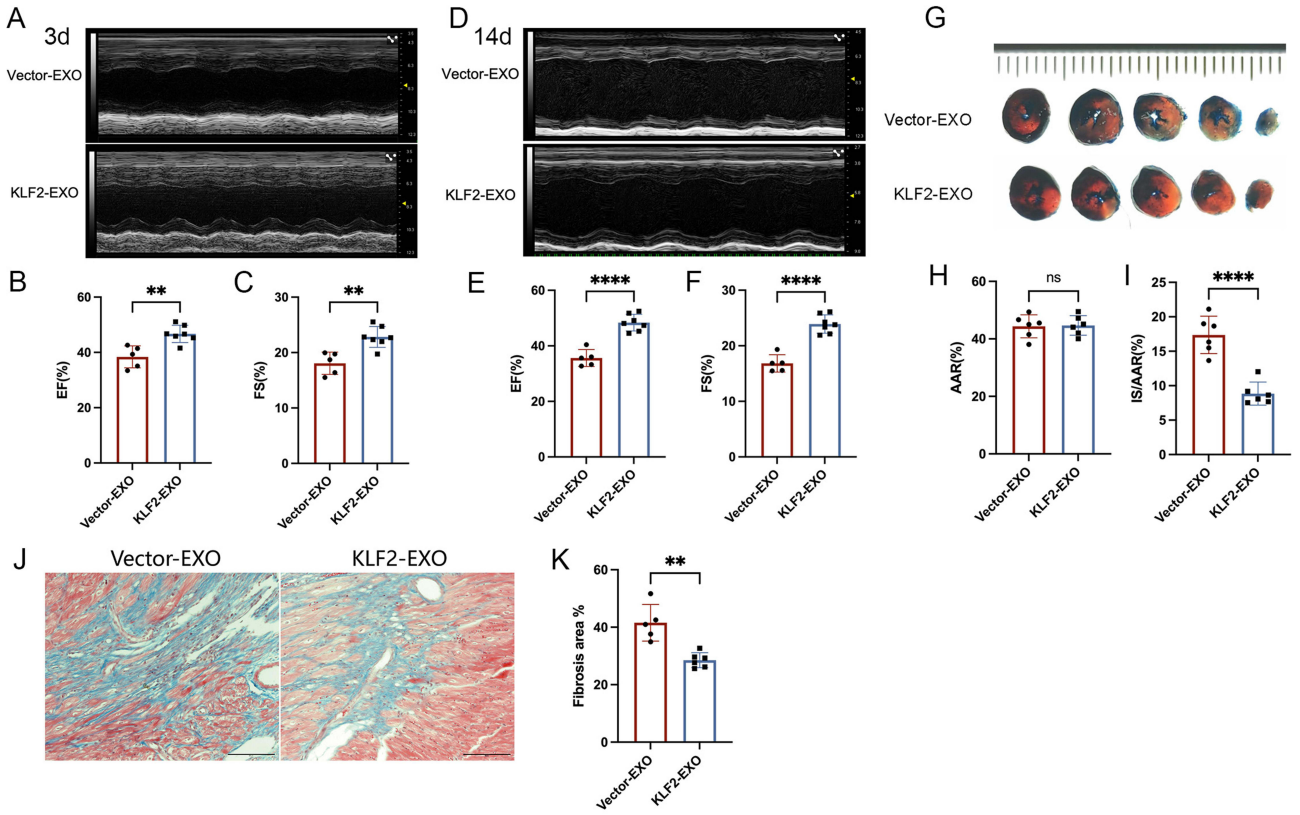

Figure 3 KLF2-EXO attenuated myocardial ischemia-reperfusion (I/R) injury. (**A**) Representative echocardiography M-mode images of Vector-EXO and KLF2-EXO treated mice in 3 days following myocardial I/R injury. KLF2-EXO: KLF2-transduced MCAECs derived exosomes; Vector-EXO: vector-transduced MCAECs derived exosomes; (**B** and **C**) Quantification of ejection fraction (EF) and fractional shortening (FS) of Vector-EXO and KLF2-EXO treated mice in 3 days following myocardial I/R injury (n=5 in Vector-EXO group, n=7 in KLF2-EXO group). (**D**) Representative echocardiography M-mode images of Vector-EXO and KLF2-EXO treated mice in 14 days following myocardial I/R injury. (**E** and **F**) Quantification of ejection fraction (EF) and fractional shortening (FS) of Vector-EXO and KLF2-EXO treated mice in 14 days following myocardial I/R injury (n=5 in Vector-EXO group, n=7 in KLF2-EXO group). (**G**) Representative images of hearts with Evans blue/TTC staining of Vector-EXO and KLF2-EXO treated mice in 3 days following myocardial I/R injury. Scale bar=5mm. (**H** and **I**) Quantitative analysis of the percentage of AAR/left ventricle and percentage of IS/AAR (n=6). AAR: Area-at-risk; IS: infarct size. (**J**) Representative images of Masson trichrome staining to assess fibrosis area of Vector-EXO and KLF2-EXO treated mice in 14 days following myocardial I/R injury. Scale bar=100μm. (**K**) Quantification of fibrosis area (%) in Masson trichrome staining within the ischemic heart 14 days following operation (n=5 in Vector-EXO group, n=6 in KLF2-EXO group). Graphs depict mean ± SD. Statistical significance was measured via Student's *t*-test for two groups' comparison. **P < 0.01, ****P < 0.0001, ns= not significant.

https://doi.org/10.2147/IJN.S512135

KLF2-EXO Were Transported into Heart and Inhibited Myocardiocyte Apoptosis After I/R Injury

The lymph is a systemic organ, and the lymph fluid can transport immune cells and extracellular vesicles. Exosomes were labelled with the fluorescent membrane marker CM-DiL (red) and injected into inguinal lymph nodes of mice with I/R injury. After 72 hours, we harvested the inguinal, heart, and axillary lymph nodes separately and detected red fluorescence in all three tissues in the KLF2-EXO and vector-EXO groups (Figure 4A). These data suggested that KLF2-EXO can be transported through the lymphatic system into the heart tissue.

Ischemia induces apoptosis in myocardial cells, and the inflammatory cascade exacerbates this process.[23] Therefore, the inhibition of myocardial apoptosis after I/R injury could rescue cardiac function. Next, we examined alterations in myocardiocyte apoptosis in the cardiac tissue. Immunofluorescence staining revealed that the number of MHC^+ $TUNEL^+$ cells (apoptotic myocytes) was significantly lower in KLF2-EXO-treated mice than that in vector-EXO-treated mice (Figure 4B and C). In addition, Western blotting of heart tissues on day 3 after I/R injury revealed significantly decreased expression of the apoptotic activator Bcl2 associated X (Bax) and cleaved Caspase3, which are responsible for morphological and biochemical changes in apoptosis, as well as significantly increased expression of Bcl2, which blocks the apoptotic death of cells in KLF2-EXO-treated mice (Figure 4D and G). These results revealed that the potential effects of KLF2-EXO can be ascribed to the regulation of cardiomyocyte apoptosis.

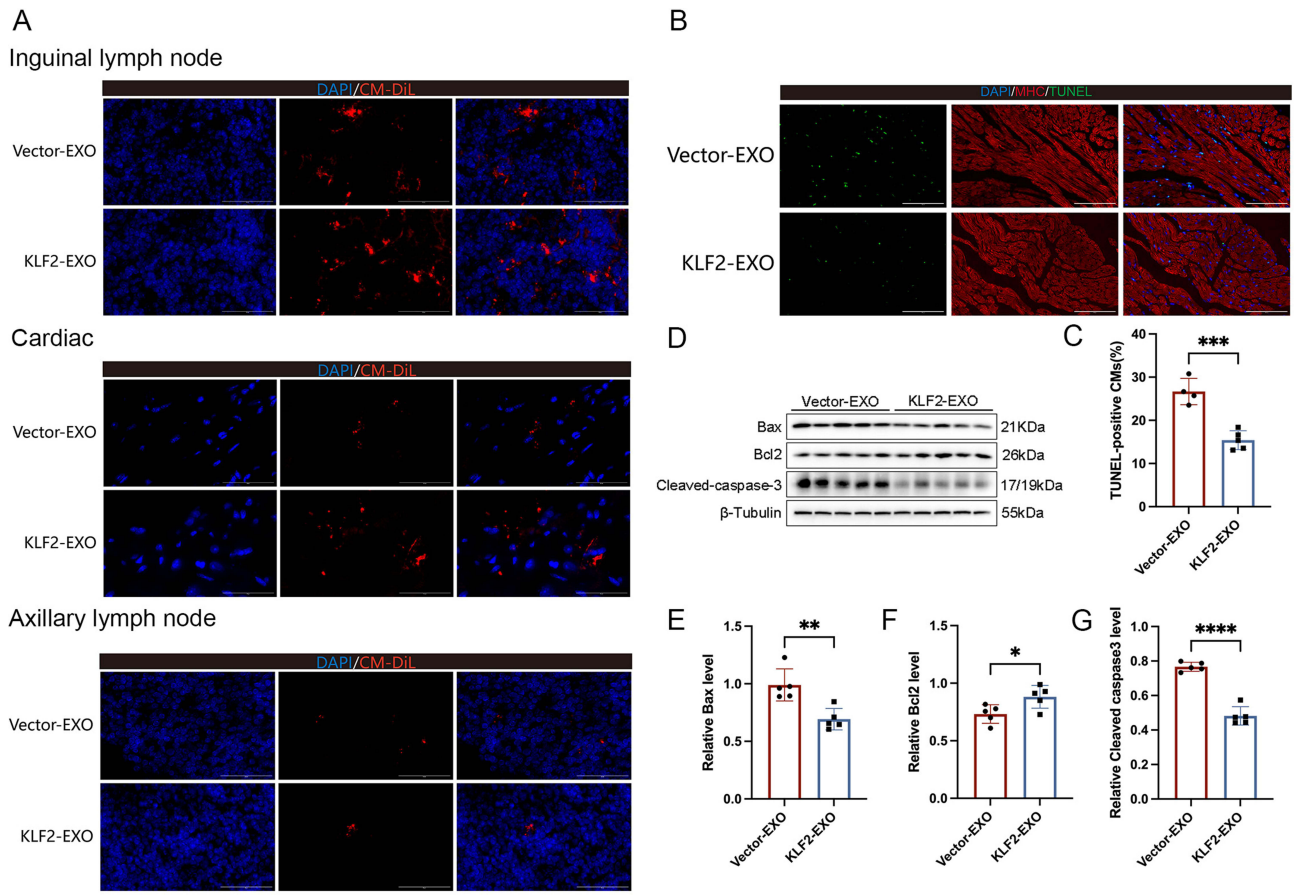

Figure 4 KLF2-EXO were transported into heart and inhibited myocardiocytes apoptosis after ischemia-reperfusion (I/R). (**A**) Representative fluorescence image of the uptake of CM-DiL-labeled exosomes (red) in inguinal lymph node, heart and axillary lymph node tissue. The nucleus was stained by DAPI (blue). (**B**) Representative fluorescence staining of TUNEL (green), MHC (red) in heart tissue of mice with Vector-EXO or KLF2-EXO treatment in 3 days following myocardial I/R injury. The nucleus was stained by DAPI (blue). KLF2-EXO: KLF2-transduced MCAECs derived exosomes; Vector-EXO: vector-transduced MCAECs derived exosomes. (**C**) Quantification of the percentage of TUNEL-positive cardiac muscle cells (CMs) in fluorescence staining (n=4 in Vector-EXO group, n=5 in KLF2-EXO group). (**D**) Representative images of Western blot to assess expression of Bax, Bcl2 and cleaved-Caspase-3 in heart tissue of mice with Vector-EXO or KLF2-EXO treatment in 3 days following myocardial I/R injury. (**E**–**G**) Quantification of expression of Bax, Bcl2 and cleaved-Caspase-3 in (**D**) (n=5). Graphs depict mean ± SD. Statistical significance was measured via Student's *t*-test for two groups' comparison. *P < 0.05, **P < 0.01, ***P < 0.001, ****P < 0.0001.

MiR-486-5p Was a Potent Candidate Mediator in KLF2-EXO′ Effect on Myocardial I/R Injury

Recent studies have reported that exosomes participate in intercellular communication via bioactive molecules including miRNAs.[24] Next, we explored whether any specific miRNAs in the KLF2-EXO exerted their effects. We carried out miRNA array analysis, and after normalization of raw sequencing data, two groups of exosomes containing three repeats were found to be highly consistent (Supplementary Material 2 for detailed data). A total of 829 miRNAs, including 805 known miRNAs (Supplementary Material 3 for detailed data), and 24 novel miRNAs were detected. Taking the fold change, P value, and mean expression level into consideration, we found that 96 miRNAs were differentially expressed, with 40 miRNAs upregulated and 56 miRNAs downregulated expression in KLF2-EXO compared to vector-EXOs (Figure 5A and B, Supplementary Material 4 for detailed data). The volcano plot (Figure 5B) clearly revealed that the expression of miR-486-5p was the most

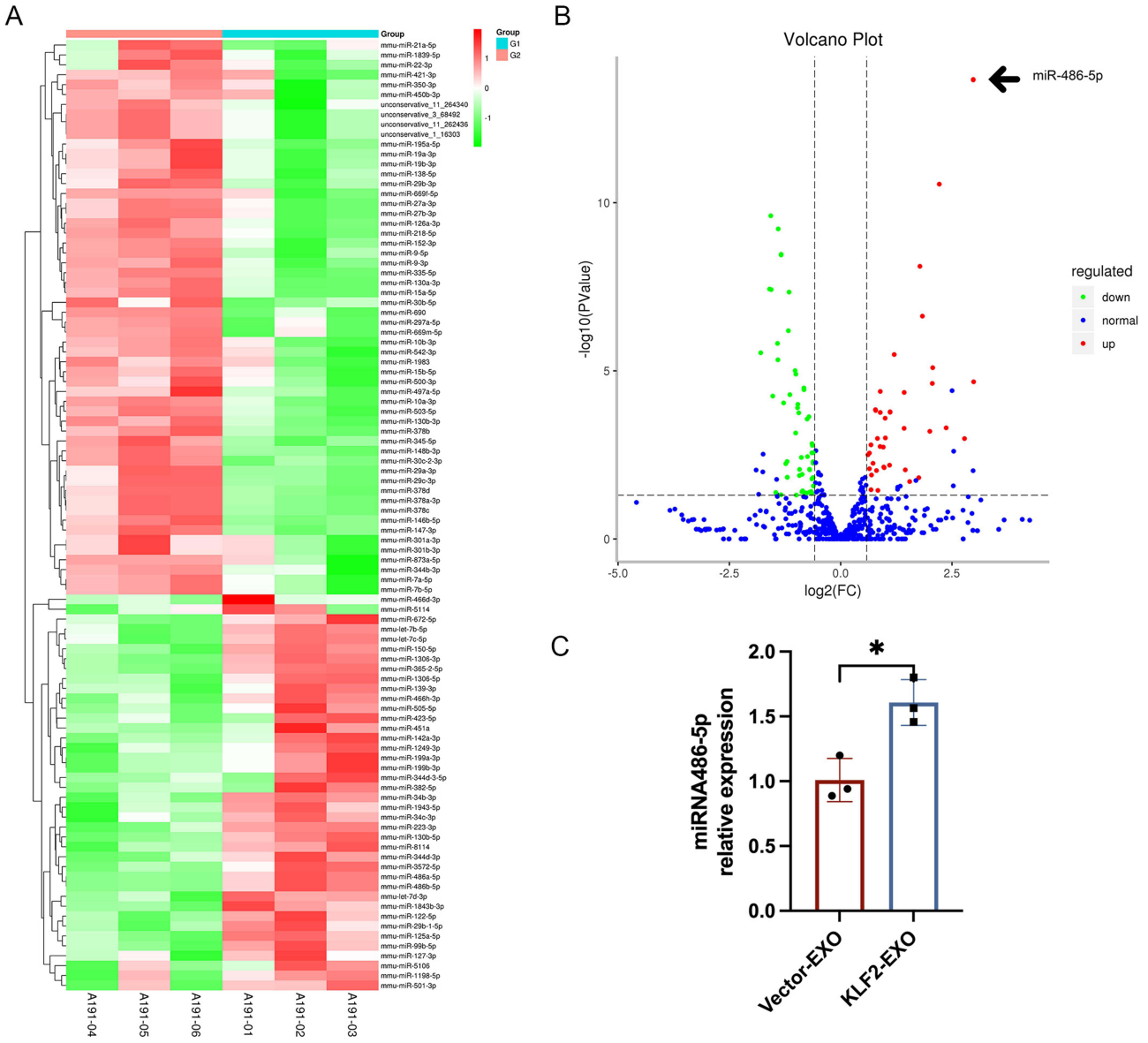

Figure 5 MiR-486-5p was potent candidate mediator in KLF2-EXO′ effect on myocardial ischemia-reperfusion (I/R) injury. (**A**) Heatmap plot of differentially expressed miRNAs in KLF2-EXO and Vector-EXO clusters (n=3). A191-01, A191-02 and A191-03 are KLF2-EXO samples (G1). A191-04, A191-05 and A191-06 are Vector-EXO samples (G2). KLF2-EXO: KLF2-transduced MCAECs derived exosomes; Vector-EXO: vector-transduced MCAECs derived exosomes. (**B**) Volcano plot showing the level of expression of the differentially expressed miRNAs from KLF2-EXO compared to Vector-EXO. The black arrow pointed miR-486-5p [log2(fold change) =2.9773, -log10 (PValue)=14]. (**C**) Quantification of miR-486-5p in KLF2-EXO compared to Vector-EXO (n=3). Statistical significance was measured via Student's *t*-test for two groups' comparison. *P < 0.05.

https://doi.org/10.2147/IJN.S512135

significantly different, with a greater fold change (log2(fold change) =2.9773, -log10 (P value) =14). Based on previous studies,[25] miR-486-5p was selected for further analysis (Supplementary Material 5). MiR-486-5p was confirmed to be more abundant in KLF2-EXO than Vector-EXO in vector-EXOs (Figure 5C).

MiR-486-5p Antagomir Abolished the Effect of KLF2-EXO on Attenuating Myocardial I/R Injury

To determine whether the cardioprotective effects of KLF2-EXO depended on miR-486-5p, we used an miR-486-5p antagomir or negative control (NC) antagomir to transfect KLF2-MCAECs and isolated exosomes from the supernatants of cultured cells. Next, we injected exosomes into inguinal lymph nodes immediately after reperfusion and assessed the extent of cardiac I/R injury and cardiac function between miR-486-5p antagomir-MCAEC-derived exosome-treated mice (miR-486-5p-Antagomir) and NC antagomir-MCAEC-derived exosome-treated mice (antagomir-NC). UCG data illustrated that the improvements in cardiac function, including EF and FS, on day 3 caused by KLF2-EXO were reversed by the application of the miR-486-5p antagomir but not the NC antagomir (Figure 6A–C). And the infarct size IS/AAR ratio in miR-486-5p antagomir treated mice is significantly higher than antagomir NC treated mice (Figure 6D–F). Additionally, the decrease in the expression of Bax and cleaved Caspase3 and the increase in the expression of Bcl2

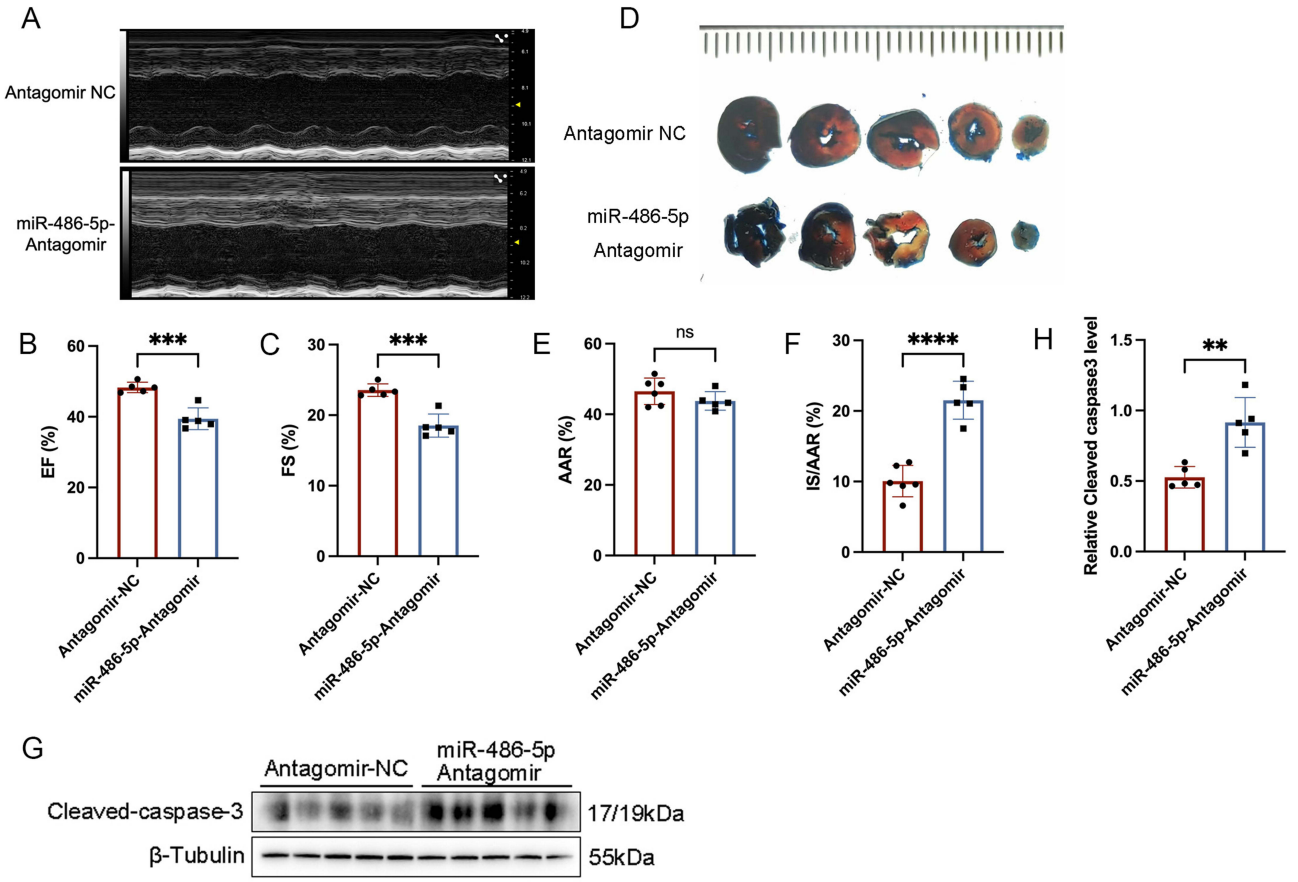

Figure 6 MiR-486-5p antagomir abrogated the effect of KLF2-EXO on ameliorating myocardial ischemia-reperfusion (I/R) injury. (**A**) Representative echocardiography M-mode images of Antagomir NC (negative control) and miR-486-5p-Antagomir exosomes treated mice in 3 days following myocardial I/R injury. (**B** and **C**) Quantification of ejection fraction (EF) and fractional shortening (FS) of Antagomir NC and miR-486-5p-Antagomir exosomes treated mice in 3 days following myocardial I/R injury (n=5). (**D**) Representative images of hearts with Evans blue/TTC staining of Antagomir NC and miR-486-5p-Antagomir exosomes treated mice in 3 days following myocardial I/R injury. Scale bar=5mm. (**E** and **F**) Quantitative analysis of the percentage of AAR/left ventricle and percentage of IS/AAR (n=6 in Antagomir-NC group, n=5 in miR-486-5p-Antagomir group). AAR: Area-at-risk; IS: infarct size. (**G**) Representative images of Western blot to assess expression of cleaved-Caspase-3 in heart tissue of mice with Antagomir NC and miR-486-5p-Antagomir exosomes treatment in 3 days following myocardial I/R injury. (**H**) Quantification of expression of cleaved-Caspase-3 in (**G**) (n=5). Graphs depict mean ± SD. Statistical significance was measured via Student's *t*-test for two groups' comparison. **P < 0.01, ***P < 0.001, ****P < 0.0001, ns= not significant.

in the heart tissue were attenuated by pretreatment with miR-486-5p antagomir (Figure 6G and H). These data reveal that miR-486-5p contributes to the benefits of KLF2-EXO in myocardial I/R injury.

PTEN-PI3K/Akt Pathway as Downstream Mechanism Participated in Regulation of KLF2-EXO on Myocardiocytes Apoptosis

We further explored the downstream mechanism by which miR-486-5p in KLF2-EXO affected myocardial I/R injury. Using TargetScan7.2, we predicted the potential target genes of miR-486-5p (Supplementary Material 6 for detailed data). We subsequently performed functional enrichment analysis with target genes (Figure 7A, Supplementary Materials 7 and 8 for detailed data) and focused on the apoptotic process (Supplementary Material 9 for detailed data). In combination with a previous study,[25] we selected PTEN, which is essential for apoptosis, as a potential target of miR-486-5p. We also detected reduced PTEN expression in KLF2-EXO-treated mice compared to vector-EXO-treated mice (Figure 7D and E). Next, we

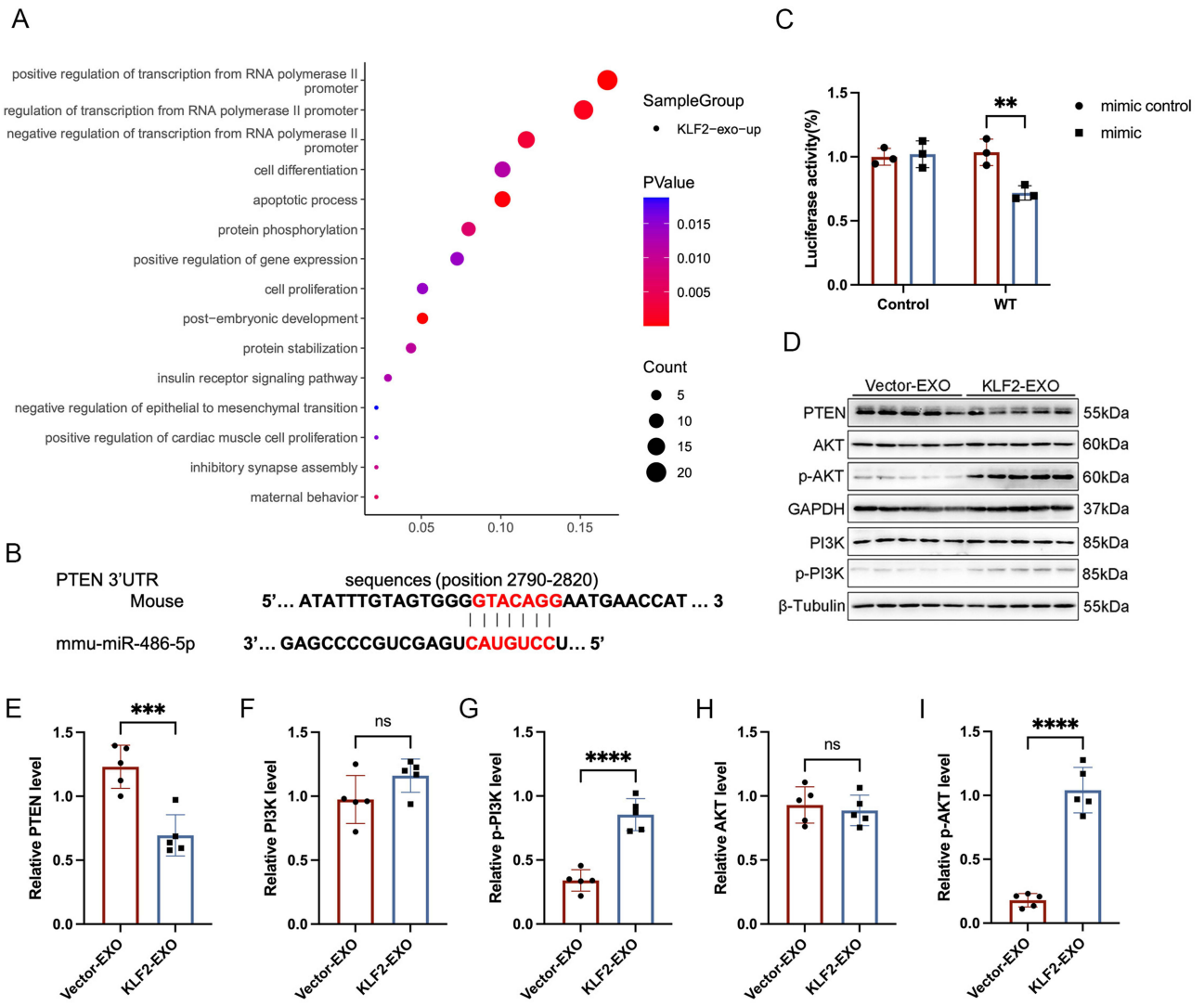

Figure 7 PTEN-PI3K/Akt pathway as downstream mechanism participated in regulation of KLF2-EXO on myocardiocytes apoptosis. (**A**) Bubble map of pathway enrichment achieved from miR-486-5p target genes with GO (Gene Ontology) enrichment analysis. (**B**) Luciferase reporter containing the mouse wild-type (WT) PTEN mRNA 3′-UTR segment and mouse miR-486-5p (mmu-miR-486-5p) sequence. The sequence in red indicates the predicted binding site for mouse miR-486-5p and PTEN mRNA. (**C**) Quantification of relative luciferase activity normalized to control (n=3). (**D**) Representative images of Western blot to assess expression of PTEN, AKT, p-AKT, PI3K, p-PI3K in heart tissue of mice with Vector-EXO or KLF2-EXO treatment in 3 days following myocardial ischemia-reperfusion (I/R) injury. KLF2-EXO: KLF2-transduced MCAECs derived exosomes; Vector-EXO: vector-transduced MCAECs derived exosomes. (**E–I**) Quantification of expression of PTEN, AKT, p-AKT, PI3K, p-PI3K in (**D**) (n=5). Graphs depict mean ± SD. Statistical significance was measured via Student's *t*-test for two groups' comparison. **P < 0.01, ***P < 0.001, ****P < 0.0001, ns= not significant.

https://doi.org/10.2147/IJN.S512135

used a dual-luciferase assay to observe the interaction between miR-486-5p and PTEN and found that the relative luciferase activity decreased in cells co-transfected with the plasmid carrying wild-type (WT)PTEN 3'UTR sequences and miR-486-5p mimics, whereas the luciferase activity in cells transfected with the control plasmid and miR-486-5p mimics remained unchanged (Figure 7B and C). These results suggested that miR-486-5p specifically binds to the 3′-UTR of PTEN mRNA. Finally, we investigated the downstream pathway of miR-486-5p-PTEN regulation. A previous study showed that overexpression of miR-486-5p, which targets PTEN, protects against coronary microembolization-induced cardiomyocyte apoptosis and improves cardiac function in rats by activating the PI3K/Akt pathway.[25] We detected the activation of PI3K and Akt proteins in KLF2-EXO-treated mice, and Western blotting of heart tissues collected on day 3 after I/R injury revealed significantly increased expression of phosphorylated PI3K and Akt (Figure 7D and F-I). These results demonstrated that the PTEN-PI3K/Akt pathway is the key regulatory component in KLF2-EXO that contributed to the inhibition of cardiomyocyte apoptosis and attenuation of myocardial I/R injury.

Discussion

Myocardial necrosis occurs in AMI when coronary blood flow decreases and insufficient oxygen supply to the heart causes cardiac ischemia.[26] Myocardial I/R injury after AMI is a critical problem in clinical practice. Reduction in myocardial apoptosis can efficiently alleviate injury.[27] In this study, we first established the use of intra-inguinal lymph node injection as a delivery pathway to exert potential therapeutic effects of KLF2-EXO in myocardial I/R injury. We subsequently highlighted that miR-486-5p, which is abundant in KLF2-EXO, inhibited myocardial apoptosis following myocardial I/R injury, whereas miR-486-5p antagomir abrogated the effect of KLF2-EXO. Finally, we found that this regulation is mediated by targeting PTEN- PI3K/Akt pathway. Thus, our study identifies a novel therapeutic strategy for I/R injury.

KLF2 is a key transcriptional regulator in ECs that is activated by the shear stress of blood in vessels and contributes to maintaining endothelial physiological conditions by inhibiting cytokine-mediated induction of E-selectin and vascular cell adhesion molecule (VCAM)-1 expression.[28,29] In our previous study, we reported that KLF2 overexpression upregulated anti-inflammatory cytokines and mimicked the physiological and anti-inflammatory phenotypes of cultured ECs.[9] Therefore, we transfected MCAECs with a lentivirus vector encoding KLF2, which resulted in a highly increase of KLF2 expression, and further experiments were performed.

Exosomes are tiny biological extracellular vesicles with membrane structures that are essential mediators of intercellular information transmission, and are widely involved in the regulation of cell function via the delivery of noncoding RNAs.[24] Previous studies have suggested that mesenchymal stem cell exosomes mediate cartilage repair by attenuating apoptosis, increasing proliferation, and modulating immune reactivity.[30] They can also reduce cardiomyocyte apoptosis under hypoxic conditions by microRNA144 via targeting the PTEN/AKT pathway.[31] Therefore, specific cell-derived exosomes could effectively regulate cardiomyocyte apoptosis. In addition, Akbar et al revealed that endothelium-derived extracellular vesicles link ischemic myocardium with monocyte mobilization and transcriptional activation following AMI via transformation of miRNA-126-3p and −5p.[32] In the current study, we confirmed KLF2-EXO attenuated myocardial I/R injury in mice by delivering miR-486-5p, which inhibited myocyte apoptosis. MiR-486-5p is enriched in muscle and highly abundant in plasma and exosomes. Preclinical studies have shown that miR-486-5p targets genes that regulate signaling pathways involved in cellular angiogenesis, proliferation, migration, and apoptosis.[33] MiR-486-5p has been validated to target PTEN and FoxO1, the suppression of which activates PI3K/Akt signaling.[34] In addition, targeting Smad1/2/4 and IGF-1 by miR-486-5p inhibits TGF-β and IGF-1 signaling,[35,36] respectively. Other miR-486-5p targets include MMP-19,[37] Sp5,[38] HAT1,[39] and NFAT5.[40] In this study, we found that miR-486-5p targets PTEN and promotes the phosphorylation of PI3K/Akt signaling, leading to the inhibition of cardiomyocyte apoptosis.

Our previous study also revealed that EVs derived from KLF2-overexpressing HUVECs containing miR-24-3p prevented $Ly6C^{high}$ monocyte recruitment from bone marrow.[9] In this study, we used exosomes derived from KLF2-overexpressing MCAECs, as well as intra-inguinal lymph node (iILN) injection, as a delivery approach to treat mice following myocardial I/R injury, and found that these exosomes reduced cardiomyocyte apoptosis and increased cardiac function by delivering miR-486-5p. Different pathways lead to the same destination, and although the two therapeutic methods involve different mechanisms, both alleviate myocardial I/R injury. Therefore, exosomes derived from KLF2-

overexpressing MCAECs may have similar functions, including prevention of $Ly6C^{high}$ monocyte recruitment through other molecular transformations. In the next step, we investigated additional mechanisms.

The lymphatic system is an entire network including vessels, nodes, and ducts that are distributed in almost all bodily tissues, which builds the circulation of lymph fluid similar to that of blood;[41] thus, it could be considered an alternative drug delivery pathway. Exosomes injected with iILN are transferred via lymphatic drainage to the target organs.[19] IILN injection has multiple advantages over IV, IC, and IM injection in terms of cost, feasibility, therapeutic retention, and IM injection methods.[42,43] Although IV and IC injections can be easily administered, a limited number of exosomes are transferred to the heart. IM injection has a more effective therapeutic effect; however, it is expensive and invasive, with a complicated system and thoracotomy. IILN injection can be implemented with a minimally invasive procedure using only a fine needle, but it yields prolonged retention and myocardial distribution of therapeutics. In addition, previous CT/PET imaging studies have revealed the existence of a mediastinal lymph node (MLN)-heart axis in AMI patients;[44] thus, lymph containing therapeutic exosomes can flow rapidly to mediastinal lymph nodes and pericardial cavities in response to cardiac injuries, exerting regulatory effects. Other studies have shown that intrapericardial exosome therapy dampens cardiac injury by activating Foxo3 and building a regulatory T cell-inducing niche in mediastinal lymph nodes.[45] We aimed to perform an intraperitoneal injection of exosomes to determine whether they would achieve improved effectiveness.

Our study had several limitations. Although the miR-486-5p antagomir reversed the effects of KLF2-EXO, the specific mechanisms should be investigated in $PTEN^{-/-}$ mice. Additionally, extracellular vesicles derived from another type of KLF2-overexpressed endothelial cells can also play important roles in attenuating myocardial I/R injury via another signaling pathway.[9] In the future, we will explore the broad effects of KLF2 overexpression on cardiac I/R injury. Additionally, the predominant sites of exosome clearance are the spleen and liver,[46] and a large volume of exosomes must be injected into the lymph nodes to confirm that exosomes are sufficient to exert their effect. Therefore, we will begin a new study to modify exosomes, which can help them escape phagocytosis and degradation in the circulation. We aimed to determine its protective effect at a low dose and its wide clinical application in patients with AMI.

Conclusions

Our study demonstrated that intra-lymph node injection of KLF2-transduced MCAE-derived exosomes improves cardiac function and inhibits myocardiocyte apoptosis in mice following myocardial I/R injury. We also provide evidence that miR-486-5p packaged in exosomes is involved in restraining myocyte apoptosis by targeting the PTEN- PI3K/Akt pathway. This study provides a new therapeutic approach involving the injection of KLF2-EXO into the lymph nodes for the treatment of myocardial I/R injury.

Data Sharing Statement

All data generated or analyzed during this study are included in the main text and Supplementary Material. Other detailed data or all the raw data used in the study are available from the corresponding author upon reasonable request.

Ethics Approval and Informed Consent

All animal experiments followed the guidelines of the Guide for the Care and Use of Laboratory Animals published by the National Institutes of Health (Eighth Edition) and were approved by the Institutional Ethics Committee of Nanjing Drum Tower Hospital (Approval No. 20011141).

Author Contributions

All authors made a significant contribution to the work reported, whether that is in the conception, study design, execution, acquisition of data, analysis and interpretation, or in all these areas; took part in drafting, revising or critically reviewing the article; gave final approval of the version to be published; have agreed on the journal to which the article has been submitted; and agree to be accountable for all aspects of the work.

Funding

This study was supported by The National Natural Science Foundation of China (grant numbers 82200299, 81870291, and 82070366).

Disclosure

The authors declare that they have no competing interests in this work.

References

1. Yeh RW, Sidney S, Chandra M, Sorel M, Selby JV, Go AS. Population trends in the incidence and outcomes of acute myocardial infarction. *N Engl J Med*. 2010;362(23):2155–2165. doi:10.1056/NEJMoa0908610
2. Ibanez B, James S, Agewall S, et al. 2017 ESC Guidelines for the management of acute myocardial infarction in patients presenting with ST-segment elevation: the Task Force for the management of acute myocardial infarction in patients presenting with ST-segment elevation of the European Society of Cardiology (ESC). *Eur Heart J*. 2018;39(2):119–177. doi:10.1093/eurheartj/ehx393
3. Yellon DM, Hausenloy DJ. Myocardial reperfusion injury. *N Engl J Med*. 2007;357(11):1121–1135. doi:10.1056/NEJMra071667
4. Frangogiannis NG. Regulation of the inflammatory response in cardiac repair. *Circ Res*. 2012;110(1):159–173. doi:10.1161/CIRCRESAHA.111.243162
5. Kain V, Prabhu SD, Halade GV. Inflammation revisited: inflammation versus resolution of inflammation following myocardial infarction. *Basic Res Cardiol*. 2014;109(6):444. doi:10.1007/s00395-014-0444-7
6. Saxena A, Russo I, Frangogiannis NG. Inflammation as a therapeutic target in myocardial infarction: learning from past failures to meet future challenges. *Transl Res*. 2016;167(1):152–166. doi:10.1016/j.trsl.2015.07.002
7. Sun X, Wei Z, Li Y, et al. Renal denervation restrains the inflammatory response in myocardial ischemia-reperfusion injury. *Basic Res Cardiol*. 2020;115(2):15. doi:10.1007/s00395-020-0776-4
8. Zhao J, Li X, Hu J, et al. Mesenchymal stromal cell-derived exosomes attenuate myocardial ischaemia-reperfusion injury through miR-182-regulated macrophage polarization. *Cardiovasc Res*. 2019;115(7):1205–1216. doi:10.1093/cvr/cvz040
9. Qiao S, Zhang W, Yin Y, et al. Extracellular vesicles derived from Krüppel-Like Factor 2-overexpressing endothelial cells attenuate myocardial ischemia-reperfusion injury by preventing Ly6C(high) monocyte recruitment. *Theranostics*. 2020;10(25):11562–11579. doi:10.7150/thno.45459
10. Chen L, Byer SH, Holder R, Wu L, Burkey K, Shah Z. Wnt10b protects cardiomyocytes against doxorubicin-induced cell death via MAPK modulation. *PLoS One*. 2023;18(10):e0277747. doi:10.1371/journal.pone.0277747
11. Godo S, Shimokawa H. Endothelial Functions. *Arterioscler Thromb Vasc Biol*. 2017;37(9):e108–e14. doi:10.1161/ATVBAHA.117.309813
12. Deanfield JE, Halcox JP, Rabelink TJ. Endothelial function and dysfunction: testing and clinical relevance. *Circulation*. 2007;115(10):1285–1295. doi:10.1161/CIRCULATIONAHA.106.652859
13. Lin Z, Kumar A, SenBanerjee S, et al. Kruppel-like factor 2 (KLF2) regulates endothelial thrombotic function. *Circ Res*. 2005;96(5):e48–57. doi:10.1161/01.RES.0000159707.05637.a1
14. He S, Wu C, Xiao J, Li D, Sun Z, Li M. Endothelial extracellular vesicles modulate the macrophage phenotype: potential implications in atherosclerosis. *Scand J Immunol*. 2018;87(4):e12648. doi:10.1111/sji.12648
15. van Niel G, D'Angelo G, Raposo G. Shedding light on the cell biology of extracellular vesicles. *Nat Rev mol Cell Biol*. 2018;19(4):213–228. doi:10.1038/nrm.2017.125
16. Zhang Y, Bi J, Huang J, Tang Y, Du S, Li P. Exosome: a Review of Its Classification, Isolation Techniques, Storage, Diagnostic and Targeted Therapy Applications. *Int J Nanomed*. 2020;15:6917–6934. doi:10.2147/IJN.S264498
17. Zhang W, Chen Z, Qiao S, et al. The effects of extracellular vesicles derived from Kruppel-Like Factor 2 overexpressing endothelial cells on the regulation of cardiac inflammation in the dilated cardiomyopathy. *J Nanobiotechnology*. 2022;20(1):76. doi:10.1186/s12951-022-01284-1
18. Natale G, Bocci G, Ribatti D. Scholars and scientists in the history of the lymphatic system. *J Anat*. 2017;231(3):417–429. doi:10.1111/joa.12644
19. Schineis P, Runge P, Halin C. Cellular traffic through afferent lymphatic vessels. *Vascul Pharmacol*. 2019;112:31–41. doi:10.1016/j.vph.2018.08.001
20. Zalewski K, Benke M, Mirocha B, Radziszewski J, Chechlinska M, Kowalewska M. Technetium-99m-based Radiopharmaceuticals in Sentinel Lymph Node Biopsy: gynecologic Oncology Perspective. *Curr Pharm Des*. 2018;24(15):1652–1675. doi:10.2174/1381612824666180515122150
21. Luo S, Truong AH, Makino A. Isolation of Mouse Coronary Endothelial Cells. *J Vis Exp*. 2016;2016(113):53985.
22. Kalluri R, LeBleu VS. The biology, function, and biomedical applications of exosomes. *Science*. 2020;367(6478):6977. doi:10.1126/science.aau6977
23. Timmers L, Pasterkamp G, de Hoog VC, Arslan F, Appelman Y, de Kleijn DP. The innate immune response in reperfused myocardium. *Cardiovasc Res*. 2012;94(2):276–283. doi:10.1093/cvr/cvs018
24. Shahabipour F, Banach M, Sahebkar A. Exosomes as nanocarriers for siRNA delivery: paradigms and challenges. *Arch Med Sci*. 2016;12(6):1324–1326. doi:10.5114/aoms.2016.62911
25. Zhu HH, Wang XT, Sun YH, et al. MicroRNA-486-5p targeting PTEN Protects Against Coronary Microembolization-Induced Cardiomyocyte Apoptosis in Rats by activating the PI3K/AKT pathway. *Eur J Pharmacol*. 2019;855:244–251. doi:10.1016/j.ejphar.2019.03.045
26. Collet JP, Thiele H, Barbato E, et al. 2020 ESC Guidelines for the management of acute coronary syndromes in patients presenting without persistent ST-segment elevation. *Eur Heart J*. 2021;42(14):1289–1367. doi:10.1093/eurheartj/ehaa575
27. Prabhu SD, Frangogiannis NG. The Biological Basis for Cardiac Repair After Myocardial Infarction: from Inflammation to Fibrosis. *Circ Res*. 2016;119(1):91–112. doi:10.1161/CIRCRESAHA.116.303577
28. Atkins GB, Jain MK. Role of Kruppel-like transcription factors in endothelial biology. *Circ Res*. 2007;100(12):1686–1695. doi:10.1161/01.RES.0000267856.00713.0a
29. Chang E, Nayak L, Jain MK. Kruppel-like factors in endothelial cell biology. *Curr Opin Hematol*. 2017;24(3):224–229. doi:10.1097/MOH.0000000000000337

30. Hade MD, Suire CN, Suo Z. Mesenchymal Stem Cell-Derived Exosomes: applications in Regenerative Medicine. *Cells*. 2021;10(8):1.
31. Wen Z, Mai Z, Zhu X, et al. Mesenchymal stem cell-derived exosomes ameliorate cardiomyocyte apoptosis in hypoxic conditions through microRNA144 by targeting the PTEN/AKT pathway. *Stem Cell Res Ther*. 2020;11(1):36. doi:10.1186/s13287-020-1563-8
32. Akbar N, Digby JE, Cahill TJ, et al. Endothelium-derived extracellular vesicles promote splenic monocyte mobilization in myocardial infarction. *JCI Insight*. 2017;2(17). doi:10.1172/jci.insight.93344.
33. Douvris A, Vinas J, Burns KD. miRNA-486-5p: signaling targets and role in non-malignant disease. *Cell mol Life Sci*. 2022;79(7):376. doi:10.1007/s00018-022-04406-y
34. Small EM, O'Rourke JR, Moresi V, et al. Regulation of PI3-kinase/Akt signaling by muscle-enriched microRNA-486. *Proc Natl Acad Sci U S A*. 2010;107(9):4218–4223. doi:10.1073/pnas.1000300107
35. Fan J, Shi S, Qiu Y, Zheng Z, Yu L. MicroRNA-486-5p down-regulation protects cardiomyocytes against hypoxia-induced cell injury by targeting IGF-1. *Int J Clin Exp Pathol*. 2019;12(7):2544–2551.
36. Ji X, Wu B, Fan J, et al. The Anti-fibrotic Effects and Mechanisms of MicroRNA-486-5p in Pulmonary Fibrosis. *Sci Rep*. 2015;5(1):14131. doi:10.1038/srep14131
37. Li Q, Xu Y, Lv K, et al. Small extracellular vesicles containing miR-486-5p promote angiogenesis after myocardial infarction in mice and nonhuman primates. *Sci Transl Med*. 2021;13(584). doi:10.1126/scitranslmed.abb0202.
38. Lu Y, Wen H, Huang J, et al. Extracellular vesicle-enclosed miR-486-5p mediates wound healing with adipose-derived stem cells by promoting angiogenesis. *J Cell mol Med*. 2020;24(17):9590–9604. doi:10.1111/jcmm.15387
39. Liu D, Zhang M, Xie W, et al. MiR-486 regulates cholesterol efflux by targeting HAT1. *Biochem Biophys Res Commun*. 2016;472(3):418–424. doi:10.1016/j.bbrc.2015.11.128
40. Duan YR, Chen BP, Chen F, et al. LncRNA lnc-ISG20 promotes renal fibrosis in diabetic nephropathy by inducing AKT phosphorylation through miR-486-5p/NFAT5. *J Cell mol Med*. 2021;25(11):4922–4937. doi:10.1111/jcmm.16280
41. Hu D, Li L, Li S, et al. Lymphatic system identification, pathophysiology and therapy in the cardiovascular diseases. *J mol Cell Cardiol*. 2019;133:99–111. doi:10.1016/j.yjmcc.2019.06.002
42. Krylova SV, Feng D. The Machinery of Exosomes: biogenesis, Release, and Uptake. *Int J mol Sci*. 2023;24(2). doi:10.3390/ijms24021337
43. Liang Y, Duan L, Lu J, Xia J. Engineering exosomes for targeted drug delivery. *Theranostics*. 2021;11(7):3183–3195. doi:10.7150/thno.52570
44. Rieckmann M, Delgobo M, Gaal C, et al. Myocardial infarction triggers cardioprotective antigen-specific T helper cell responses. *J Clin Invest*. 2019;129(11):4922–4936. doi:10.1172/JCI123859
45. Zhu D, Liu S, Huang K, et al. Intrapericardial Exosome Therapy Dampens Cardiac Injury via Activating Foxo3. *Circ Res*. 2022;131(10):e135–e50. doi:10.1161/CIRCRESAHA.122.321384
46. Kimiz-Gebologlu I, Oncel SS. Exosomes: large-scale production, isolation, drug loading efficiency, and biodistribution and uptake. *J Control Release*. 2022;347:533–543. doi:10.1016/j.jconrel.2022.05.027